Dyes and Pigments 90 (2011) 211–218

Contents lists available at ScienceDirect

Dyes and Pigments

journal homepage: www.elsevier.com/locate/dyepig

Short communication

Synthesis and near-infrared absorption properties of linearly π-extended squarylium oligomers

Shigeyuki Yagi [a,*], Yuuki Nakasaku [a], Takeshi Maeda [a], Hiroyuki Nakazumi [a], Yoshiaki Sakurai [b]

[a] Department of Applied Chemistry, Graduate School of Engineering, Osaka Prefecture University, 1-1 Gakuen-cho, Naka-ku, Sakai, Osaka 599-8531, Japan
[b] Environment and Chemistry Department, Technology Research Institute of Osaka Prefecture, 2-7-1 Ayumino, Izumi, Osaka 594-1157, Japan

ARTICLE INFO

Article history:
Received 13 October 2010
Received in revised form
6 December 2010
Accepted 7 December 2010
Available online 15 December 2010

Keywords:
Squarylium
Oligomer
NIR dye
Low band gap
Absorption spectra
π-Conjugation system

ABSTRACT

Linear squarylium oligomers bearing extended π-conjugation systems were newly synthesized, and their near-infrared (NIR) light-absorbing properties were investigated. Replacement of the iodo substituent in a 5-iodinated indolino-squarylium dye to the 2-hydroxy-3,4-dioxocyclobut-1-en-1-yl functional group *via* the Pd-catalyzed cross-coupling with a tributylstannylsquarate followed by condensation with a quaternary indolium salt afforded the semi-squarylium-attached squarylium derivative, *i.e.*, the squarylium dimer. The introduction of the semi-squarylium unit gave rise to a significant bathochromic shift towards the NIR region ($\lambda_{abs} = 763$ nm in $CHCl_3$ at 298 K). Starting from a 5,5′-diiodinated indolino-squarylium, the iterative extension of semi-squarylium units successfully yielded the linearly π-extended trimer and pentamer, that showed absorption maxima at 862 and 940 nm in $CHCl_3$ at 298 K, respectively. Especially, the pentamer exhibited a considerably low optical band gap of 1.1 eV.

1. Introduction

Squaryliums, often called squaraines, are well-known functional dyes because their unique optical properties such as intense light absorption and moderately efficient fluorescence emission in visible-to-NIR regions are useful for various applications; chemosensors and chemodosimeters for various chemicals [1–7], noncovalent fluorescent probes for bioanalyses [8–12], organic light-emitting diodes [13,14], supramolecular architectures [15–18], and so on. In the last decade, squaryliums have also received increasing attention as photosensitizers in dye-sensitized solar cells [19–23] because their excellent electron donating properties along with large light absorptivity are suitable for the sensitization of a TiO_2 nanocrystalline electrode *via* the photo-induced electron transfer mechanism [24].

Another valuable property of squaryliums is the photoconductivity in the solid states [25]. Various types of symmetrical and unsymmetrical squaryliums have been prepared by Law and coworkers [26–29], and their photoconductive properties were enthusiastically investigated towards application as photoreceptors in xerographic devices [30–32]. Such a unique optoelectronic property has also made them applicable to thin-film organic photovoltaic devices. Indeed, p-n heterojunction solar cells [33,34] as well as bulk-heterojunction solar cells [35–37] have been developed using squarylium-based organic semiconductors. The semiconductive behaviour of squaryliums is believed to be based on well-organized stacking of the intramolecular donor–acceptor–donor structure consisting of a cyclobutene core with aromatic/heterocyclic components at both ends. Varying the aromatic/heterocyclic components allows us to tune the optical and electronic properties of squaryliums.

Nowadays, squarylium-derived molecules bearing low optical band gaps receive considerable attention because they are expected to work well in the field of organic photovoltaics to harvest sunlight in the NIR regions. Although several types of squarylium-based low optical band gap polymers have so far been reported [38–40], further investigation on new synthetic strategies is eagerly required to obtain various types of squarylium-based π-extended chromophores [41,42]. We have so far reported the syntheses of various types of NIR-absorbing squaryliums and related chromophores, as shown in Fig. 1a; unsymmetrical squaryliums [43], methine-bridged bis-squaryliums [44–46], and bis-squarylium dyes with π-spacers [47,48]. These synthetic protocols have opened the door to novel squarylium-based π-extended chromophores with low optical band gaps. In the present study, we show a new approach to construct squarylium-based π-conjugation systems,

---

* Corresponding author. Tel.: +81 72 254 9324; fax: +81 72 254 9910.
E-mail address: yagi@chem.osakafu-u.ac.jp (S. Yagi).

0143-7208/$ – see front matter © 2010 Elsevier Ltd. All rights reserved.
doi:10.1016/j.dyepig.2010.12.005

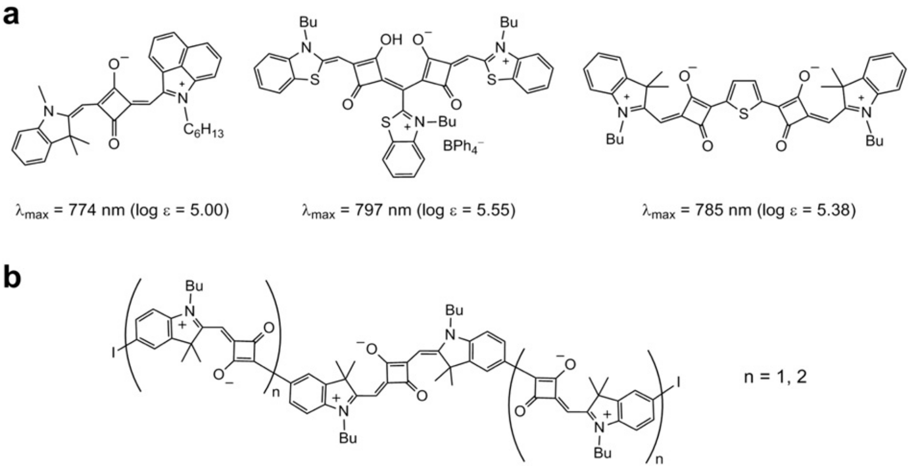

Fig. 1. Structures of π-extended squarylium derivatives; (a) unsymmetrical squarylium and symmetrically π-extended bis-squaryliums, and (b) linearly π-extended bis-squaryliums targeted in the present study.

that is, the synthesis of novel linearly π-extended squarylium oligomers (Fig. 1b).

2. Results and discussion

2.1. Synthesis and light-absorbing properties of lineary π-extended squarylium dimers

First, we attempted to develop the linear dimeric squarylium **LSQ-1**, bearing two cyclobutene cores and three dimethylindoline components (Scheme 1), because this is the minimum extension of the squarylium array in the present system. The key reaction is the introduction of a squaric acid moiety on the iodinated site of the indole ring in the squarylium precursor **2**. We obtained **2** by the stepwise unsymmetrical squarylium synthesis employing a semi-squarylium precursor **1** [43,49]. Then, according to the Liebeskind's method [50], **2** was successfully reacted with the tributylstannylsquarate **3** under Pd-catalyzed conditions to afford the squarate-attached squarylium **4** in 65% yield, which was hydrolyzed to the corresponding squaric acid derivative **5** under acidic conditions (67%). The subsequent condensation with a heterocyclic quaternary salt under typical conditions for squarylium synthesis was expected to afford **LSQ-1**. Indeed, the reaction of **5** with 1-butyl-2,3,3-trimethylindolium iodide under azeotropic conditions (1-butanol–benzene, reflux) in the presence of a small amount of quinoline afforded the desired linear dimer **LSQ-1** in 50% yield, the structure of which was characterized by ^{1}H NMR, IR, and HRMS spectra.

In Fig. 2 are shown the Vis-NIR absorption spectra of **2**, **4**, and **LSQ-1** in $CHCl_3$ at 298 K, and the detailed data are summarized in Table 1. The squarylium **2** exhibits intense absorption at 642 nm with a molar absorption coefficient (ε_{abs}) of 2.34×10^5 M^{-1} cm^{-1}. This spectral profile is similar to that of the unsubstituted symmetrical indolino-squarylium dye, except for a 12 nm bathochromic shift of the absorption maximum (λ_{abs}) [51]. Thus, the iodo substituent in **2** has little influence on the light absorption property of the indolino-squarylium dye. On the other hand, when a squarate moiety is introduced in place of the iodo group,

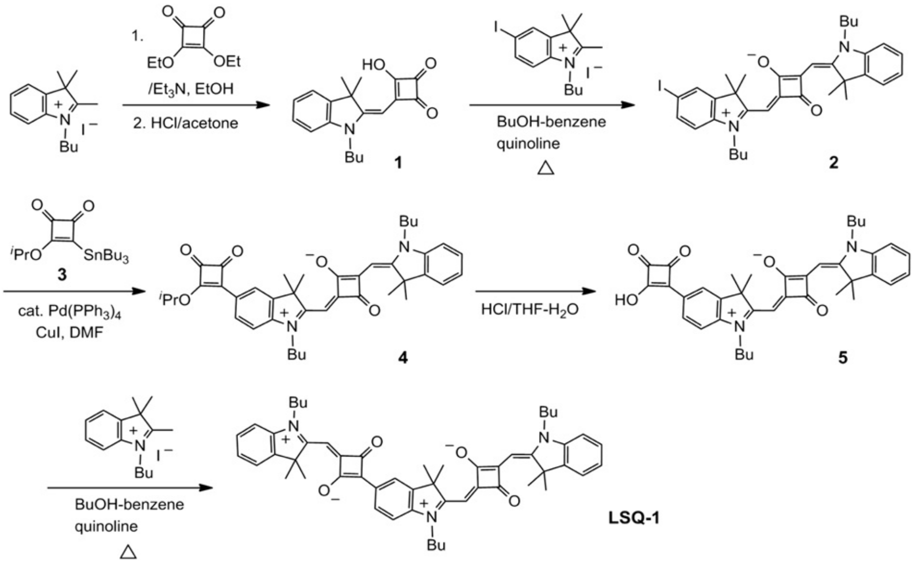

Scheme 1.

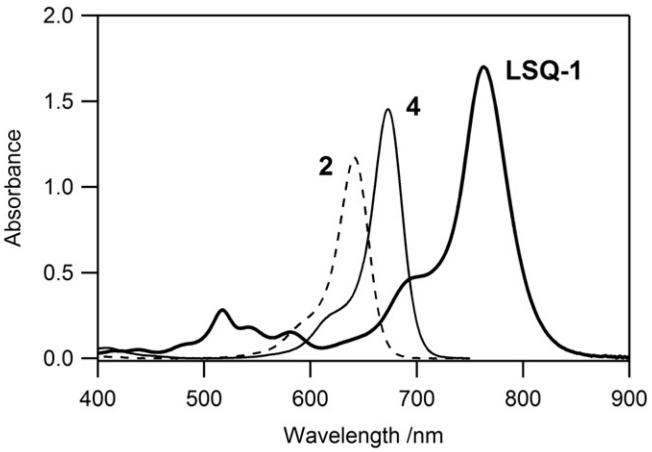

Fig. 2. Vis-NIR absorption spectra of **2** (dashed), **4** (plain), and **LSQ-1** (bold) in $CHCl_3$ at 298 K. Dye concentrations are adjusted to 5.0 μM.

a bathochromic shift of *ca*. 30 nm is observed for **4**, the ε_{abs} of which is still large (2.91×10^5 M^{-1} cm^{-1}). In the case of **LSQ-1**, an additional bathochromic shift is observed, and the λ_{abs} reaches the NIR region ($\lambda_{max} = 763$ nm, $\varepsilon_{abs} = 3.40 \times 10^5$ M^{-1} cm^{-1}). This should be attributed to the additional semi-squarylium moiety that gives rise to the extension of the π-conjugated system. Although fluorescent properties are also investigated for **LSQ-1**, it exhibited little fluorescent emission in common organic solvents.

In order to investigate the effect of the attached semi-squarylium moiety on the electronic absorption, density functional theory (DFT) calculations were performed for **LSQ-1**, using a Spartan '08 program package (Wavefunction, Inc., Irvine, California) [52]. In order to simplify the calculations, the *N*-butyl groups were replaced by methyls, and the structure was fully optimized at the B3LYP/6-31G** level. The frontier molecular orbitals are shown in Fig. 3. The HOMO is localized mainly on the core of the squarylium backbone, and quite low electron density is distributed on the semi-squarylium moiety. On the other hand, the electron density on the semi-squarylium moiety significantly increases at the LUMO level. This result indicates that the HOMO-LUMO excitation gives rise to significant intramolecular charge transfer from the squarylium to the attached semi-squarylium moiety, resulting in intense light absorption in the NIR region.

2.2. Synthesis and light-absorbing properties of lineary extended squarylium trimer and pentamer

The achievement of the synthesis of **LSQ-1** enabled us to prepare the symmetrically π-extended oligomeric squaryliums **LSQ-2** and **LSQ-3** (Fig. 1b, $n = 1$ and 2, respectively) by iteration of introduction of the squarate moieties followed by condensation with the indolium salts. Towards this purpose, the diiodinated squarylium **6** was employed as the starting material. As shown in Scheme 2, the reaction of **6** with tributylstannylsquarate **3** followed by hydrolysis afforded the doubly squarate-substituted squarylium **8**, that reacted with 2 mol eq. of 1-butyl-5-iodo-2,3,3-trimethylindolium iodide to give the trimeric squarylium **LSQ-2**. The subsequent squarate functionalization of **LSQ-2** was also achieved to afford **10** *via* **9**, from which finally the pentameric squarylium oligomer **LSQ-3** could be obtained. The structures of **LSQ-2** and **LSQ-3** were characterized by ^1H NMR, IR, and HRMS spectra. Especially, the ^1H NMR spectra offered valuable information about the extension of the semi-squarylium units. In Fig. 4 are shown the expanded regions of ^1H NMR spectra of **6**, **LSQ-2**, and **LSQ-3**. The ^1H signal patterns indicate that both **LSQ-2** and **LSQ-3** possess highly symmetrical structures. In the spectrum of **LSQ-2**, two methine protons, four *N*-methylene protons, and six aromatic protons are additionally observed in comparison with the spectrum of **6**. This clearly shows that the semi-squarylium units are attached at both ends of **6**. Similarly, in the spectrum of **LSQ-3**, the ^1H signal patterns in the methine, *N*-methylene and aromatic regions suggest further extention of semi-squarylium moieties from **LSQ-2**. From these results, the indolino-squarylium π-conjugation system was successfully extended by iterative introduction of semi-squarylium moieties.

Table 1
Electronic absorption data of squarylium derivatives ($CHCl_3$, 298 K).

Compd	λ_{abs}/nm	ε_{abs}/M^{-1} cm^{-1}
2	642	234000
4	673	291000
LSQ-1	763	340000
6	649	272000
7	694	378000
LSQ-2	862	357000
9	905	343000
LSQ-3	940	371000

In Fig. 5 are shown the Vis-NIR spectra of **6**, **LSQ-2**, and **LSQ-3** in $CHCl_3$ at 298 K. The data are also summarized in Table 1. The λ_{abs} of **6** was observed at 649 nm with the ε_{abs} of 2.72×10^5 M^{-1} cm^{-1}, almost corresponding to that of **2**. When two semi-squarylium moieties were introduced to **6** to obtain **LSQ-2**, the λ_{max} was bathochrmically shifted to 862 nm with an enlarged ε_{abs}

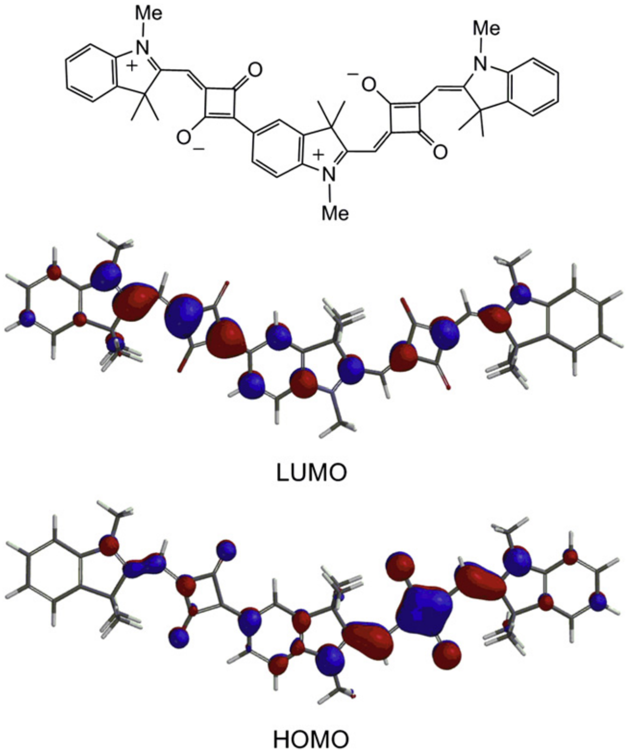

Fig. 3. The frontier molecular orbitals of *N*-methyl analogue of **LSQ-1** obtained by DFT calculations using the B3LYP/6-31G** basis set ($E_{HOMO} = -4.5078$ eV, $E_{LUMO} = -2.7057$ eV).

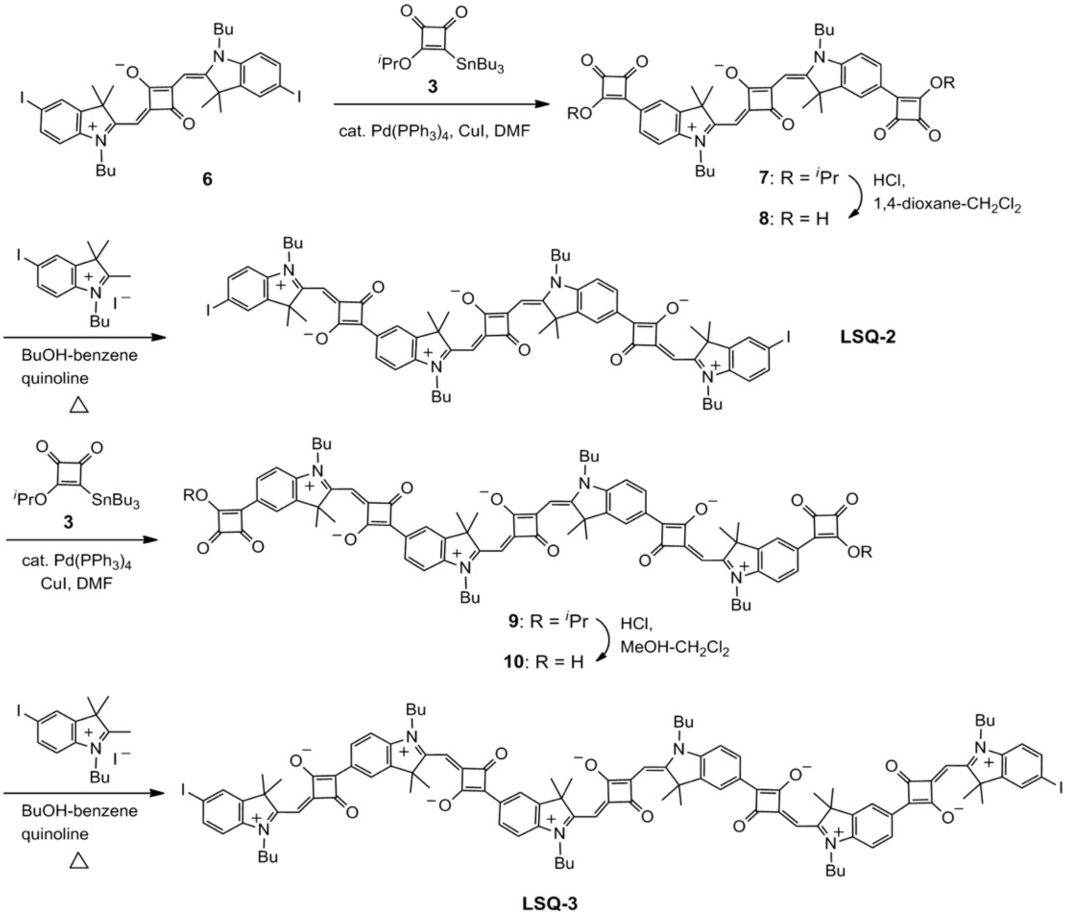

Scheme 2.

(3.57×10^5 M^{-1} cm^{-1}). Further extension of the semi-squarylium units, as demonstrated in **LSQ-3**, gave rise to a considerable bathochromic shift up to 940 nm. It is worth noting that the absorption edge of **LSQ-3** reaches 1100 nm, showing a HOMO-LUMO band gap of 1.1 eV. Such a low optical band gap squarylium is very rare, except for polymeric squaryliums [38–40,53]. In Fig. 6 is shown the relationship between λ_{max} and ε_{abs} in **LSQ-1**–**3**. It is obvious that the extension of the π-conjugation system leads to the increase in ε_{abs} to enhance the oscillator strength of the squarylium oligomer. Therefore, the present synthetic protocol towards linear oligomeric squaryliums should offer lots of opportunities to develop squarylium-based π-conjugation systems applicable as NIR-optoelectronics materials.

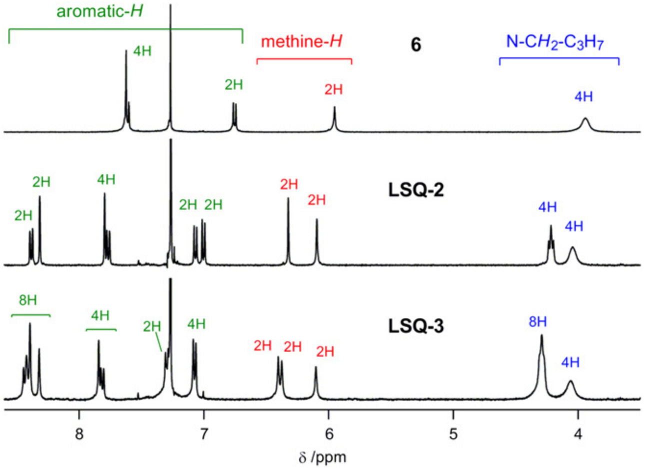

Fig. 4. Expanded regions of ^{1}H NMR spectra of **6**, **LSQ-2**, and **LSQ-3** obtained in $CDCl_3$ at 298 K.

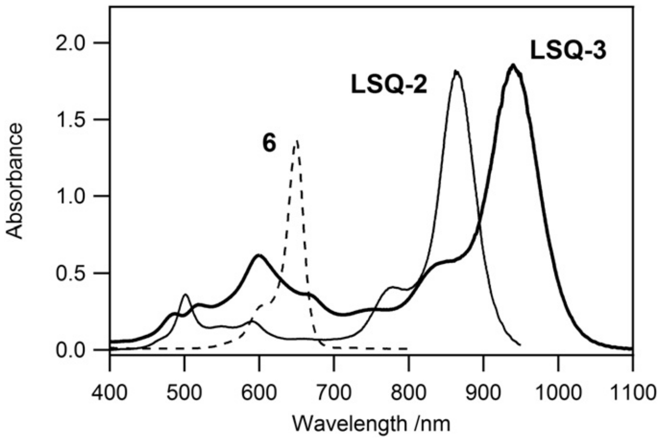

Fig. 5. Vis-NIR absorption spectra of **6** (dashed), **LSQ-2** (plain), and **LSQ-3** (bold) in $CHCl_3$ at 298 K. Dye concentrations are adjusted to 5.0 μM.

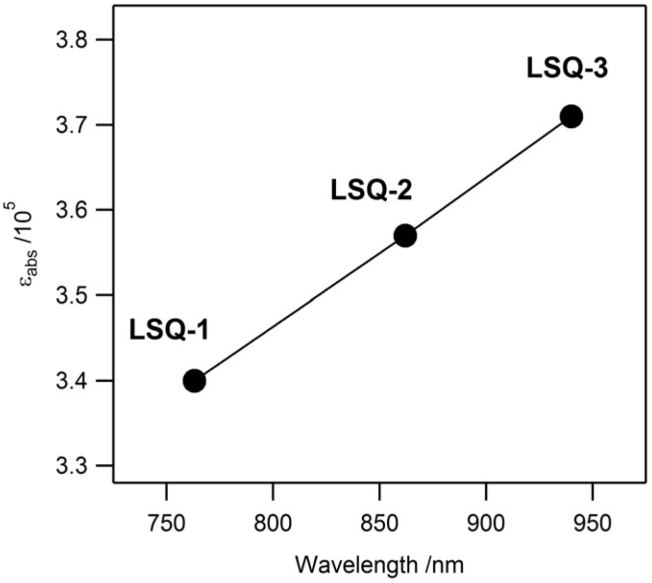

Fig. 6. The plots of the molar absorption coefficients (ε_{abs}) versus absorption maxima (λ_{max}) for **LSQ-1**–**3**.

3. Conclusions

In conclusion, we here demonstrated the synthesis of novel oligomeric squaryliums. Repeating the introduction of squarate moieties into the iodinated sites of the indolino-squarylium followed by condensation with a 1-butyl-2,3,3-trimethyl indolium salt allowed us to extend the π-conjugation by semi-squarylium units in a linear manner. Using other aromatic and/or heterocyclic components, heterolytically linked squarylium oligomers should be prepared to tune optical and electronic properties. Using squarylium oligomers, fabrication of photovoltaic devices is also currently undergoing and will be reported elsewhere in near future.

4. Experimental

4.1. General

The ^{1}H NMR spectra were obtained on a Jeol JNM LA-400 spectrometer, using TMS as an internal standard (0.00 ppm). The IR spectra were obtained as KBr pellets on a Shimadzu FT-IR 8400S spectrophotometer. The Vis-NIR absorption and fluorescence emission spectra were obtained on a Shimadzu UV-3100 spectrophotometer and a Shimadzu RF-5000 spectrofluorometer, respectively, where chloroform of spectroscopic grade was used as a solvent. MALDI-TOF mass analyses were performed on a Shimadzu Kratos KOMPACT MALDI2 spectrometer, using sinapinic acid as a matrix. High resolution mass analyses were performed on a Jeol JMS-SX-102A mass spectrometer (fast atom bombardment ionization, FAB), using 3-nitrobenzylalcohol as a matrix. Elemental analyses were performed on a Yanaco CHN CORDER MT-3 analyzer.

For preparation of **LSQ-1**, squarylium **2** was prepared according to the stepwise synthesis of an unsymmetrical squarylium already reported [43,49]. For preparation of **LSQ-2** and **LSQ-3**, squarylium **6** was prepared from 1-butyl-5-iodo-2,3,3-trimethylindolium iodide and squaric acid (3,4-dihydroxy-3-cyclobutene-1,2-dione) according to the conventional squarylium synthesis [51]. Squaric acid was purchased from Tokyo Chemical Industry co., ltd, and used without purification. 3-(1-Methyl)ethyloxy-4-tributylstannylcyclobut-3-ene-1,2-dione **3** was prepared according to the literature [50]. For reversed phase column chromatography, octadodecyl end-capped silica gel (COSMOSIL 75C18-OPN, Nacalai Tesque, Inc.) was used.

4.2. Preparation of ***LSQ-1***

4.2.1. Compound **4**

In a two-necked 50 mL round-bottom flask equipped with a condenser, squarylium **2** (0.50 g, 0.77 mmol) was dissolved in 10 mL of DMF under N_2 atmosphere. To the solution were added tributylstannylsquarate **3** (0.57 g, 1.3 mmol), $Pd(PPh_3)_4$ (0.072 g, 0.062 mmol), and CuI (0.012 g, 0.063 mmol), and the mixture was stirred at 45 °C for 20 h under N_2 atmosphere. After cooling, the solvent was removed on a rotary evaporator, and the residue was purified by silica gel column chromatography (eluent; $CHCl_3$/AcOEt/hexane, 4/2/1, v/v/v). Further purification was carried out by recrystallization, the crystals being grown by slow diffusion from a $CHCl_3$ solution to hexane. Finally, **4** was obtained in 65% yield as a green solid (0.32 g, 0.50 mmol); ^{1}H NMR (400 MHz, $CDCl_3$) δ 8.05 (d, $J = 7.8$ Hz, 1H, Ar—H), 7.95 (s, 1H, Ar—H), 7.40 (d, $J = 7.8$ Hz, 1H, Ar—H), 7.36 (t, $J = 7.8$ Hz, 1H, Ar—H), 7.23 (t, $J = 7.8$ Hz, 1H, Ar—H), 7.08 (d, $J = 7.8$ Hz, 1H, Ar—H), 7.00 (d, $J = 7.8$ Hz, 1H, Ar—H), 6.09 (s, 1H, methine-H), 6.01 (s, 1H, methine-H), 5.63 (sept, $J = 5.9$ Hz, 1H, O$CH(CH_3)_2$), 4.09 (t, $J = 7.3$ Hz, 2H, N—CH_2—), 3.95 (t, $J = 7.3$ Hz, 2H, N—CH_2—), 1.81 (m, 16H, —$CH_2CH_2CH_2CH_3$ and $C(CH_3)_2$), 1.58 (d, $J = 5.9$ Hz, 6H, $OCH(CH_3)_2$), 1.48 (m, 4H, —$CH_2CH_2CH_2CH_3$), 1.01 (m, 6H, —$CH_2CH_2CH_2CH_3$); IR (KBr) 2957, 2868, 1778, 1738, 1601, 1501, 1356, 1277, 1186, 1076 cm^{-1}; MALDI-TOF MS (m/z) 646 ([M]$^+$).

4.2.2. Compound **5**

In a two-necked 100 mL round-bottom flask equipped with a condenser, **4** (0.10 g, 0.15 mmol) was dispersed in a mixture of 25 mL of THF and 9 mL of 8 M HCl. The mixture was stirred at 40 °C for 24 h under N_2 atmosphere. After cooling, the solvent was removed by distillation under reduced pressure, the temperature being kept below 40 °C. The residue was purified by reversed phase column chromatography (eluent; MeOH/H_2O, 4/1, v/v) to afford **5** in 67% yield as a green solid (0.061 g, 0.10 mmol), which was used in the next step without further purification; ^{1}H NMR (400 MHz, CD_3OD) δ 8.18–8.15 (m, 2H, Ar—H), 7.48 (d, $J = 7.8$ Hz, 1H, Ar—H), 7.35 (d, $J = 7.8$ Hz, 1H, Ar—H), 7.30–7.17 (m, 3H, Ar—H), 6.04 (s, 1H, methine-H), 5.98 (s, 1H, methine-H), 4.18–4.08 (m, 4H, N—CH_2—), 1.89–1.72 (m, 16H, —$CH_2CH_2CH_2CH_3$ and $C(CH_3)_2$), 1.57–1.48 (m, 4H, —$CH_2CH_2CH_2CH_3$), 1.06–1.02 (m, 6H, —$CH_2CH_2CH_2CH_3$) (the OH signal was not observed due to rapid proton exchange); IR (KBr) 3429, 2951, 2866, 1757, 1583, 1499, 1398, 1354, 1279, 1186, 1088 cm^{-1}; MALDI-TOF MS (m/z) 604 ([M]$^+$).

4.2.3. Squarylium dimer ***LSQ-1***

In a two-necked 50 mL round-bottom flask equipped with a condenser and a Dean—Stark distillation apparatus, **5** (0.045 g, 0.074 mmol) and 1-butyl-2,3,3-trimethylindolium iodide (0.14 g, 0.41 mmol) were dissolved in a mixture of 12 mL of 1-butanol and 3 mL of benzene. Then, a few drops of quinoline were added, and the mixture was heated at reflux for 6 h under N_2 atmosphere, where water generated during the reaction was azeotropically removed. After cooling, the solvent was removed on a rotary evaporator, and the residue was purified by silica gel column chromatography (eluent; $CHCl_3$/AcOEt/MeOH, 24/4/3, v/v/v). Further purification was carried out by recrystallization, the crystals being grown by slow diffusion from a CH_2Cl_2 solution to cyclohexane. Finally, **LSQ-1** was obtained in 50% yield as a green solid (0.030 g, 0.037 mmol); ^{1}H NMR (400 MHz, $CDCl_3$) δ 8.36 (d, $J = 7.8$ Hz, 1H, Ar—H), 8.29 (s, 1H, Ar—H), 7.51 (d, $J = 7.8$ Hz, 1H, Ar—H), 7.45 (t, $J = 7.8$ Hz, 1H, Ar—H), 7.39–7.24 (m, 4H, Ar—H), 7.19 (t, $J = 7.8$ Hz, 1H, Ar—H), 7.05–7.00 (m, 2H, Ar—H), 6.33 (s, 1H, methine-H), 6.05, (s, 1H, methine-H), 6.01 (s, 1H, methine-H), 4.24–4.28 (t, $J = 7.8$ Hz, 2H, $N{-}CH_2{-}$), 4.05 (br, 2H, $N{-}CH_2{-}$), 3.98 (br, 2H, $N{-}CH_2{-}$), 1.93–1.75 (m, 24H, $-CH_2CH_2CH_2CH_3$ and $C(CH_3)_2$), 1.57–1.43 (m, 6H, $-CH_2CH_2CH_2CH_3$), 1.05–0.95 (m, 9H, $-CH_2CH_2CH_2CH_3$); IR (KBr) 2951, 2866, 1738, 1605, 1558, 1497, 1454, 1387, 1271, 1182, 1084 cm^{-1}; HRMS (FAB) calcd for $C_{53}H_{59}N_3O_4$: 801.4506 (M^+, 100%). Found: 801.4442.

4.3. *Preparation of **LSQ-2** and **LSQ-3***

4.3.1. *Compound **7***

In a two-necked 50 mL round-bottom flask equipped with a condenser, squarylium **6** (0.50 g, 0.66 mmol) was dissolved in 15 mL of DMF under N_2 atmosphere. To the solution were added **3** (0.85 g, 2.0 mmol), $Pd(PPh_3)_4$ (0.12 g, 0.10 mmol), and CuI (0.020 g, 0.11 mmol), and the mixture was stirred at 45 °C for 20 h under N_2 atmosphere. After cooling, a colored precipitate was formed, which was collected by filtration. The obtained solid was washed with small amounts of AcOEt and hexane, and further purification was carried out by recrystallization, the crystals being grown by slow diffusion from a $CHCl_3$ solution to hexane. Finally, **7** was obtained in 62% yield as a green solid (0.32 g, 0.41 mmol); ^1H NMR (400 MHz, $CDCl_3$) δ 8.08 (d, $J = 8.3$ Hz, 2H, Ar–H), 8.00 (s, 2H, Ar–H), 7.10 (d, $J = 8.3$ Hz, 2H, Ar–H), 6.10 (s, 2H, methine-H), 5.64 (sept, $J = 6.3$ Hz, 2H, $OCH(CH_3)_2$), 4.03 (br, 4H, $N{-}CH_2{-}$) 1.83 (m, 16H, $-CH_2CH_2CH_2CH_3$ and $C(CH_3)_2$), 1.59 (d, $J = 6.3$ Hz, 12H, $OCH(CH_3)_2$), 1.47 (sext, $J = 7.3$ Hz, 4H, $-CH_2CH_2CH_2CH_3$), 1.01 (t, $J = 7.3$ Hz, 6H, $-CH_2CH_2CH_2CH_3$); IR (KBr) 2943, 2782, 1740, 1604, 1497, 1393, 1350, 1342, 1269, 1177, 1065 cm^{-1}; MALDI-TOF MS (*m/z*) 785 ($[M + H]^+$).

4.3.2. *Compound **8***

In a two-necked 100 mL round-bottom flask equipped with a condenser, **7** (0.50 g, 0.64 mmol) was dispersed in a mixture of 10 mL of 1,4-dioxane, 8 mL of CH_2Cl_2 and 3.5 mL of 4 M HCl. The mixture was stirred at 60 °C for 24 h under N_2. After cooling, a colored precipitate was collected by filtration. The solvent was removed by distillation under reduced pressure, the temperature being kept below 40 °C. The obtained solid was washed with small amounts of AcOEt and hexane to afford **8** in 56% yield as a green solid (0.25 g, 0.36 mmol), which was used in the next step without further purification; ^1H NMR (400 MHz, DMSO-d_6) δ 9.08 (s, 2H, OH), 8.04 (s, 2H, Ar–H), 7.92 (d, $J = 8.3$ Hz, 2H, Ar–H), 6.99 (d, $J = 8.3$ Hz, 2H, Ar–H), 5.66 (s, 2H, methine-H), 4.01 (br, 4H, $N{-}CH_2{-}$), 1.69 (quint, 16H, $-CH_2CH_2CH_2CH_3$), 1.61 (s, 12H, $C(CH_3)_2$), 1.40 (sext, $J = 7.3$ Hz, 4H, $-CH_2CH_2CH_2CH_3$), 0.94 (t, $J = 7.3$ Hz, 6H, $-CH_2CH_2CH_2CH_3$); IR (KBr) 3479, 2936, 1782, 1767, 1605, 1558, 1489, 1385, 1346, 1273, 1180, 1088 cm^{-1}; MALDI-TOF MS (*m/z*) 701 ($[M + H]^+$).

4.3.3. *Squarylium trimer **LSQ-2***

In a two-necked 50 mL round-bottom flask equipped with a condenser and a Dean–Stark distillation apparatus, **8** (0.42 g, 0.60 mmol) and 1-butyl-5-iodo-2,3,3-trimethylindolium iodide (1.18 g, 2.5 mmol) were dissolved in a mixture of 8 mL of 1-butanol and 2 mL of benzene. Then, a few drops of quinoline were added, and the mixture was heated at reflux for 5 h under N_2 atmosphere, where water generated during the reaction was azeotropically removed. After cooling, the solvent was removed on a rotary evaporator, and the residue was purified by silica gel column chromatography (eluent; $CHCl_3$/AcOEt/MeOH, 10/10/1, v/v/v). Further purification was carried out by recrystallization, the crystals being grown by slow diffusion from a $CHCl_3$ solution to hexane. Finally, **LSQ-2** was obtained in 27% yield as a green solid (0.22 g, 0.16 mmol); ^1H NMR (400 MHz, $CDCl_3$) δ 8.38 (d, $J = 8.3$ Hz, 2H, Ar–H), 8.32 (s, 2H, Ar–H), 7.80 (s, 2H, Ar–H), 7.77 (d, $J = 8.3$ Hz, 2H, Ar–H), 7.07 (d, $J = 8.3$ Hz, 2H, Ar–H), 7.00 (d, $J = 8.3$ Hz, 2H, Ar–H), 6.31 (s, 2H, methine-H), 6.09 (s, 2H, methine-H), 4.21 (t, $J = 7.3$ Hz, 4H, $N{-}CH_2{-}$), 4.05 (br, 4H, $N{-}CH_2{-}$), 1.86–1.84 (m, 32H, $-CH_2CH_2CH_2CH_3$ and $C(CH_3)_2$), 1.52–1.45 (m, 8H, $-CH_2CH_2CH_2CH_3$), 1.04–0.99 (m, 12H, $-CH_2CH_2CH_2CH_3$); IR (KBr) 2937, 1612, 1604, 1558, 1489, 1435, 1396, 1339, 1261, 1177, 1088, 1042 cm^{-1}. HRMS (FAB) calcd for $C_{72}H_{76}I_2N_4O_6$: 1346.3854 (M^+, 100%). Found: 1346.3800.

4.3.4. *Compound **9***

In a two-necked 50 mL round-bottom flask equipped with a condenser, **LSQ-2** (0.087 g, 0.065 mmol) was dissolved in 3 mL of DMF under N_2 atmosphere. To the solution was added **3** (0.090 g, 0.21 mmol), $Pd(PPh_3)_4$ (0.006 g, 0.005 mmol), and CuI (0.001 g, 0.005 mmol), and the mixture was stirred at 45 °C for 1 h under N_2 atmosphere. After cooling, a colored precipitate was formed, which was collected by filtration. The obtained solid was washed with small amounts of AcOEt and hexane, and further purification was carried out by recrystallization, the crystals being grown by slow diffusion from a $CHCl_3$ solution to hexane. Finally, a green solid of **9** was obtained in 68% yield (0.060 g, 0.044 mmol); ^1H NMR (400 MHz, $CDCl_3$) δ 8.41 (d, $J = 8.3$ Hz, 2H, Ar–H), 8.34 (s, 2H, Ar–H), 8.17 (d, $J = 8.3$ Hz, 2H, Ar–H), 8.09 (s, 2H, Ar–H), 7.34 (d, $J = 8.3$ Hz, 2H, Ar–H), 7.09 (m, 4H d, $J = 8.3$ Hz, 2H, Ar–H), 6.39 (s, 2H, methine-H), 6.12 (s, 2H, methine-H), 5.66 (sept, $J = 6.3$ Hz, 2H, $OCH(CH_3)_2$), 4.27 (t, $J = 7.3$ Hz, 4H, $N{-}CH_2{-}$), 4.06 (br, 4H, $N{-}CH_2{-}$), 1.93–1.79 (m, 32H, $-CH_2CH_2CH_2CH_3$ and $C(CH_3)_2$), 1.61 (d, $J = 6.3$ Hz, 12H, $OCH(CH_3)_2$), 1.54–1.44 (m, 8H, $-CH_2CH_2CH_2CH_3$), 1.05–1.01 (m, 12H, $-CH_2CH_2CH_2CH_3$); IR (KBr) 2939, 1782, 1747, 1605, 1543, 1489, 1435, 1396, 1339, 1261, 1173, 1072, 1038 cm^{-1}; MALDI-TOF MS (*m/z*) 1372 ($[M + H]^+$).

4.3.5. *Compound **10***

In a two-necked 100 mL round-bottom flask equipped with a condenser, **9** (0.045 g, 0.033 mmol) was dispersed in a mixture of 12 mL of $CHCl_3$, 6 mL of MeOH and 0.6 mL of 6 M HCl. The mixture was stirred at 70 °C for 24 h under N_2 atmosphere. After cooling, the solvent was removed on a rotary evaporator, and the residue was washed with MeOH and water. The obtained solid was thoroughly dried under reduced pressure to obtain **10** in 82% yield as a green solid (0.035 g, 0.027 mmol), which was used in the next step without further purification; ^1H NMR (400 MHz, DMSO-d_6) δ 8.17–8.12 (m, 8H, Ar–H), 7.82 (d, $J = 8.3$ Hz, 2H, Ar–H), 7.50 (d, $J = 8.3$ Hz, 2H, Ar–H), 6.29 (s, 2H, methine-H), 5.93 (s, 2H, methine-H), 4.43 (br, 4H, $N{-}CH_2{-}$), 4.14 (br, 4H, $N{-}CH_2{-}$), 1.90–1.68 (m, 32H, $-CH_2CH_2CH_2CH_3$ and $C(CH_3)_2$), 1.47–1.36 (m, 8H, $-CH_2CH_2CH_2CH_3$), 0.98–0.93 (m, 12H, $-CH_2CH_2CH_2CH_3$); IR (KBr) 3441, 2939, 1774, 1767, 1605, 1558, 1488, 1435, 1396, 1342, 1265, 1177, 1092, 1034 cm^{-1}; MALDI-TOF MS (*m/z*) 1287 ($[M + H]^+$).

4.3.6. *Squarylium pentamer **LSQ-3***

In a two-necked 50 mL round-bottom flask equipped with a condenser and a Dean–Stark distillation apparatus, **10** (0.21 g, 0.16 mmol) and 1-butyl-2,3,3-trimethylindolium iodide (0.22 g, 64 mmol) was dissolved in a mixture of 12 mL of 1-butanol and 3 mL of benzene. Then, a few drops of quinoline were added, and the mixture was heated at reflux for 1 h under N_2 atmosphere, where water generated during the reaction was azeotropically removed. After cooling, the solvent was removed on a rotary evaporator, and the residue was purified by silica gel column chromatography (eluent; $CHCl_3$/AcOEt/MeOH, 10/3/2, v/v/v). Further purification was carried out by recrystallization, the crystals being grown by slow diffusion from a $CHCl_3$ solution to hexane. Finally, **LSQ-3** was obtained in 11% yield as a green solid (0.034 g, 0.018 mmol); ^1H NMR (400 MHz, $CDCl_3$) δ 8.44–8.39 (m, 6H, Ar–H), 8.32 (s, 2H, Ar–H), 7.84 (s, 2H, Ar–H), 7.80 (d, $J = 8.3$ Hz, 2H, Ar–H), 7.29 (d, $J = 8.3$ Hz, 2H, Ar−H), 7.07 (d, $J = 8.3$ Hz, 4H, Ar−H), 6.40, (s, 2H, methine-H), 6.37 (s, 2H, methine-H), 6.10 (s, 2H, methine-H), 4.29 (m, 8H, $\mathrm{N{-}C}H_2{-}$), 4.06 (m, 4H, $\mathrm{N{-}C}H_2{-}$), 1.91−1.84 (m, 48H, $-\mathrm{CH_2C}H_2\mathrm{CH_2CH_3}$ and $\mathrm{C(C}H_3)_2$), 1.55−1.42 (m, 12H, $-\mathrm{CH_2CH_2C}H_2\mathrm{CH_3}$), 1.05−1.00 (m, 18H, $-\mathrm{CH_2CH_2CH_2C}H_3$); IR (KBr) 2939, 1747, 1604, 1558, 1489, 1435, 1396, 1339, 1258, 1173, 1076, 1041 $\mathrm{cm^{-1}}$. HRMS (FAB) calcd for $\mathrm{C_{110}H_{114}I_2N_6O_{10}}$: 1933.6686 ($\mathrm{M^+}$, 100%). Found: 1933.2764.

References

[1] Yagi S, Hyodo Y, Hirose M, Nakazumi H, Sakurai Y, Ajayaghosh A. Metallo supramolecular assemblies of bis-squaraines by allosteric $\mathrm{Ca^{2+}}$ ion binding. Organic Letters 2007;9(10):1999–2002.

[2] Ros-Lis JV, Martinez-Manez R, Soto J. Colorimetric signaling of large aromatic hydrocarbons via the enhancement of aggregation processes. Organic Letters 2005;7(12):2337–9.

[3] Ros-Lis JV, Marcos MD, Martinez-Manez R, Rurack K, Soto J. A regenerative chemodosimeter based on metal-induced dye formation for the highly selective and sensitive optical determination of $\mathrm{Hg^{2+}}$ ions. Angewandte Chemie International Edition 2005;44(28):4405–7.

[4] Arunkumar E, Ajayaghosh A, Daub J. Selective calcium ion sensing with a bichromophoric squaraine foldamer. Journal of the American Chemical Society 2005;127(9):3156–64.

[5] Ros-Lis JV, Martinez-Manez R, Rurack K, Sancenon F, Soto J, Spieles M. Highly selective chromogenic signaling of $\mathrm{Hg^{2+}}$ in aqueous media at nanomolar levels employing a squaraine-based reporter. Inorganic Chemistry 2004;43(17):5183–5.

[6] Oguz U, Akkaya EU. A squaraine-based sodium selective fluorescent chemosensor. Tetrahedron Letters 1998;39(32):5857–60.

[7] Chenthamarakshan CR, Ajayaghosh A. Enhanced sensitivity and selectivity in lithium ion recognition property of an oligomeric squaraine dye based fluorescent sensor. Tetrahedron Letters 1998;39(13):1795–8.

[8] Yan WY, Sloat AL, Yagi S, Nakazumi H, Colyer CL. Protein labeling with red squarylium dyes for analysis by capillary electrophoresis with laser-induced fluorescence detection. Electrophoresis 2006;27(7):1347–54.

[9] Jisha VS, Arun KT, Hariharan M, Ramaiah D. Site-selective binding and dual mode recognition of serum albumin by a squaraine dye. Journal of the American Chemical Society 2006;128(18):6024–5.

[10] Xiang ZM, Nesterov EE, Skoch J, Lin T, Hyman BT, Swager TM, et al. Detection of myelination using a novel histological probe. Journal of Histochemistry and Cytochemistry 2005;53(12):1511–6.

[11] Welder F, Paul B, Nakazumi H, Yagi S, Colyer CL. Symmetric and asymmetric squarylium dyes as noncovalent protein labels: a study by fluorimetry and capillary electrophoresis. Journal of Chromatography B-Analytical Technologies in the Biomedical and Life Sciences; 2003:93–105.

[12] Nakazumi H, Colyer CL, Kaihara K, Yagi S, Hyodo Y. Red luminescent squarylium dyes for noncovalent HSA labeling. Chemistry Letters; 2003:804–5.

[13] Matsui M, Tanaka S, Funabiki K, Kitaguchi T. Synthesis, properties, and application as emitters in organic electroluminescence devices of quinacridone- and squarylium-dye-centred dendrimers. Bulletin of the Chemical Society of Japan 2006;79(1):170–6.

[14] Mori T, Kim HG, Mizutani T, Lee DC. Electroluminescent properties in organic light-emitting diode doped with two guest dyes. Japanese Journal of Applied Physics Part 1-Regular Papers Short Notes & Review Papers 2001;40(9A):5346–9.

[15] Fu N, Baumes JM, Arunkumar E, Noll BC, Smith BD. Squaraine rotaxanes with boat conformation macrocycles. Journal of Organic Chemistry 2009;74(17):6462–8.

[16] Gassensmith JJ, Arunkumar E, Barr L, Baumes JM, DiVittorio KM, Johnson JR, et al. Self-assembly of fluorescent inclusion complexes in competitive media including the interior of living cells. Journal of the American Chemical Society 2007;129(48):15054–9.

[17] Ajayaghosh A, Chithra P, Varghese R. Self-assembly of tripodal squaraines: cation-assisted expression of molecular chirality and change from spherical to helical morphology. Angewandte Chemie International Edition 2007;46(1–2):230–3.

[18] Arunkumar E, Forbes CC, Noll BC, Smith BD. Squaraine-derived rotaxanes: sterically protected fluorescent near-IR dyes. Journal of the American Chemical Society 2005;127(10):3288–9.

[19] Kuster S, Sauvage F, Nazeeruddin MK, Grätzel M, Nuesch FA, Geiger T. Unsymmetrical squaraine dimer with an extended p-electron framework: an approach in harvesting near infra-red photons for energy conversion. Dyes and Pigments 2010;87(1):30–8.

[20] Mor GK, Kim S, Paulose M, Varghese OK, Shankar K, Basham J, et al. Visible to near-infrared light harvesting in $\mathrm{TiO_2}$ nanotube array-P3HT based heterojunction solar cells. Nano Letters 2009;9(12):4250–7.

[21] Geiger T, Kuster S, Yum JH, Moon SJ, Nazeeruddin MK, Grätzel M, et al. Molecular design of unsymmetrical squaraine dyes for high efficiency conversion of low energy photons into electrons using $\mathrm{TiO_2}$ nanocrystalline films. Advanced Functional Materials 2009;19(17):2720–7.

[22] Yum JH, Walter P, Huber S, Rentsch D, Geiger T, Nüesch F, et al. Efficient far red sensitization of nanocrystalline $\mathrm{TiO_2}$ films by an unsymmetrical squaraine dye. Journal of the American Chemical Society 2007;129(34):10320–1.

[23] Burke A, Schmidt-Mende L, Ito S, Grätzel M. A novel blue dye for near-IR 'dye-sensitised' solar cell applications. Chemical Communications 2007;(3):234–6.

[24] Ushiroda S, Ruzycki N, Lu Y, Spitler MT, Parkinson BA. Dye sensitization of the anatase (101) crystal surface by a series of dicarboxylated thiacyanine dyes. Journal of the American Chemical Society 2005;127(14):5158–68.

[25] Law KY. Organic photoconductive materials–Rcent trends and developments. Chemical Reviews 1993;93(1):449–86.

[26] Law KY, Bailey FC. Squaraine chemistry–synthesis, characterization, and optical properties of a class of novel unsymmetrical squaraines - 4-(Dimethylamino)phenyl (4′-methoxyphenyl)squaraine and its derivatives. Journal of Organic Chemistry 1992;57(12):3278–86.

[27] Law KY. Squaraine chemistry–design, synthesis, and xerographic properties of a highly sensitive unsymmetrical fluorinated squaraine. Chemistry of Materials 1992;4(3):605–11.

[28] Law KY, Bailey FC. A new approach to symmetrical and unsymmetrical photoconductive squaraines. Journal of the Chemical Society-Chemical Communications 1991;(17):1156–8.

[29] Law KY, Bailey FC. Squaraine chemistry - Synthesis, characterization and xerographic properties of bis(4-methylbenzylaminophenyl)-squaraine and its derivatives. Dyes and Pigments 1988;9(2):85–107.

[30] Law KY, Facci JS, Bailey FC, Yanus JF. Squaraine chemistry–solution electrochemistry and its use in assessing the relative photosensitivity of squaraines in bilayer xerographic devices. Journal of Imaging Science 1990;34(2):31–8.

[31] Law KY, Bailey FC. Squaraine chemistry–Effect of synthesis on the morphological and xerographic properties of photoconductive squaraines. Journal of Imaging Science 1987;31(4):172–7.

[32] Law KY. Effects of fabrication and aging on the xerographic properties of squaraine photoconductive devices. Journal of Imaging Science 1987;31(3):83–93.

[33] Morel DL, Ghosh AK, Feng T, Stogryn EL, Purwin PE, Shaw RF, et al. High-efficiency organic solar cells. Applied Physics Letters 1978;32(8):495–7.

[34] Merritt VY, Hovel HJ. Organic solar cells of hydroxy squarylium. Applied Physics Letters 1976;29(7):414–5.

[35] Wei GD, Wang SY, Renshaw K, Thompson ME, Forrest SR. Solution-processed squaraine bulk heterojunction photovoltaic cells. ACS Nano 2010;4(4):1927–34.

[36] Bagnis D, Beverina L, Huang H, Silvestri F, Yao Y, Yan H, et al. Marked alkyl- vs alkenyl-substitutent effects on squaraine dye solid-state structure, carrier mobility, and bulk-heterojunction solar cell efficiency. Journal of the American Chemical Society 2010;132(12):4074–5.

[37] Silvestri F, Irwin MD, Beverina L, Facchetti A, Pagani GA, Marks TJ. Efficient squaraine-based solution processable bulk-heterojunction solar cells. Journal of the American Chemical Society 2008;130(52):17640–1.

[38] Ajayaghosh A, Eldo J. A novel approach toward low optical band gap polysquaraines. Organic Letters 2001;3(16):2595–8.

[39] Ajayaghosh A, Chenthamarakshan CR, Das S, George MV. Zwitterionic dye-based conducting polymers. Synthesis and optical properties of pyrrole-derived polysquaraines. Chemistry of Materials 1997;9(3):644–6.

[40] Havinga EE, Tenhoeve W, Wynberg H. A new class of small band-gap organic polymer conductors. Polymer Bulletin 1992;29(1–2):119–26.

[41] Ajayaghosh A. Chemistry of squaraine-derived materials: near-IR dyes, low band gap systems, and cation sensors. Accounts of Chemical Research 2005;38(6):449–59.

[42] Beverina L, Salice P. Squaraine compounds: tailored design and synthesis towards a variety of material science applications. European Journal of Organic Chemistry 2010;(7):1195–201.

[43] Yagi S, Hyodo Y, Matsumoto S, Takahashi N, Kono H, Nakazumi H. Synthesis of novel unsymmetrical squarylium dyes absorbing in the near-infrared region. Journal of the Chemical Society-Perkin Transactions 1 2000;(4):599–603.

[44] Yagi S, Nakai K, Hyodo Y, Nakazumi H. Synthesis of near-infrared absorbing bisquarylium dyes bearing unsymmetrically extended Π-conjugation structures. Synthesis-Stuttgart 2002;(3):413–7.

[45] Yagi S, Fujie Y, Hyodo Y, Nakazumi H. Synthesis, structure, and complexation properties with transition metal cations of a novel methine-bridged bisquarylium dye. Dyes and Pigments 2002;52(3):245–52.

[46] Nakazumi H, Natsukawa K, Nakai K, Isagawa K. Synthesis and structure of new cationic squarylium dyes. Angewandte Chemie International Edition 1994;33(9):1001–3.

[47] Yagi S, Ohta T, Akagi N, Nakazumi H. The synthesis and optical properties of bis-squarylium dyes bearing arene and thiophene spacers. Dyes and Pigments 2008;77(3):525–36.

[48] Yagi S, Murayama S, Hyodo Y, Fujie Y, Hirose M, Nakazumi H. Synthesis and light absorption/emission properties of novel bis-squaraine dyes with extensively conjugated π-electron systems. Journal of the Chemical Society-Perkin Transactions 1 2002;(12):1417–9.

[49] Terpetschnig E, Lakowicz JR. Synthesis and characterization of unsymmetrical squaraines - A new class of cyanine dyes. Dyes and Pigments 1993;21(3):227–34.

[50] Liebeskind LS, Fengl RW. 3-Stannylcyclobutenediones as Nucleophilic cyclobutenedione equivalents - Synthesis of substitutedcyclobutenediones and cyclobutenedione monoacetals and the beneficial effect of catalytic copper

iodide on the Stille reaction. Journal of Organic Chemistry 1990;55(19):5359–64.

[51] Sprenger HE, Ziegenbein W. The cyclobutenediylium cation, a novel chromophore from squaric acid. Angewandte Chemie International Edition 1967;6(6):553–4.

[52] Shao Y, Molnar LF, Jung Y, Kussmann J, Ochsenfeld C, Brown ST, et al. Advances in methods and algorithms in a modern quantum chemistry program package. Physical Chemistry Chemical Physics 2006;8(27):3172–91.

[53] Eldo J, Arunkumar E, Ajayaghosh A. Fluorescent bispyrroles. New building blocks for novel π-conjugated polymers. Tetrahedron Letters 2000;41(32):6241–4.